Spectroscopic Evidence for the Formation of Helical Structures in Gas-Phase Short Peptide Chains†

Valérie Brenner, François Piuzzi, Iliana Dimicoli, Benjamin Tardivel, and Michel Mons*

Laboratoire Francis Perrin, URA CEA-CNRS 2453, Service des Photons, Atomes et Molécules, CEA Saclay, bât 522, Gif-sur-Yvette Cedex, France

Received: January 26, 2007; In Final Form: April 19, 2007

Aminoisobutyric acid (Aib) is a synthetic amino acid known to favor the formation of 3_{10} helical structures in condensed phases, namely, crystals. The intrinsic character of these helicogenic properties has been investigated on the Ac-Aib-Phe-Aib-NH_2 molecule under isolated conditions, namely, in the gas phase, both experimentally by double-resonance IR/UV spectroscopy and theoretically by quantum chemistry. A convergent set of evidence, based on energetic, IR, and UV spectroscopic data as well as on analogies with the similar peptide Ac-Ala-Phe-Ala-NH_2 previously studied, enables us to conclude the formation of an incipient 3_{10} helix in these isolated systems.

1. Introduction

Optical spectroscopy of biomolecules carried out in a cold environment provides an acute insight on the most stable conformations of these species. Supersonic expansions or helium droplets provide an efficient cooling for both rotational and conformational degrees of freedom, leading to a dramatic spectral simplification compared to condensed phase spectroscopy. These approaches, combined with depopulation spectroscopic techniques,[1−7] have led to the development of single-conformation optical spectroscopy, in particular in the IR range. This has allowed spectroscopists, in particular Roger Miller and his group, to unravel the conformational diversity of several floppy molecules by distinguishing the spectral contribution of the several conformations populated.[1−7] When applied simultaneously, the several IR techniques used (IR depopulation in He droplets and IR/UV hole burning in supersonic expansions) have proven to be complementary and provide a global picture of the molecule studied.[8]

In the case of gas-phase isolated peptides, IR/UV double resonance spectroscopy is an efficient diagnostic of the H-bonding network of the system. The amide A region (around 3 μm) interrogates the NH stretches and provides direct information on the number and intensity of H-bonds.[7,9−13] The amide I and II regions, corresponding to CO stretches and NH bends, give also interesting hints on the structure, providing that theoretical calculations are available for comparison.[10,14−16]

In the past 4 years, several neutral peptides have been studied by these techniques, with, however, radically different strategies:

(i) Modified peptides are model molecules mimicking the central part of a peptide or a protein chain and whose study focuses on the intrinsic properties of the chain itself.[10,17−27] The role of the caps on both termini is to keep intact the amide groups of the chain. The goal is here to gain insights on the archetypal structures of a peptide backbone, in particular on the competition between the different types of folding, which are essentially controlled by the ability of the amide NH moieties to bind to a more or less remote carbonyl group, giving rise to the so-called C_7 and C_{10} H-bonds (Figure 1).[7,18] Evidence for the spontaneous formation of different types of secondary structures in the gas phase have been reported recently, namely, γ-turns,[10,17,22,26,27] β-turns,[20,25] helical 3_{10}[23] structures in peptide chains, or model β-sheets in dimers[9,10] of capped peptides. So far the size of the species studied did not go beyond three residues, and so far no C_{13} H bond could be observed in these model systems.

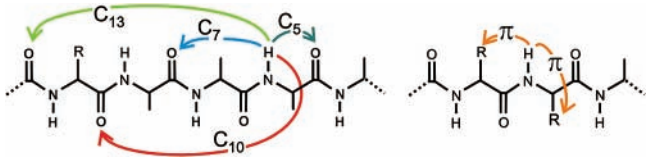

Figure 1. Scheme of the sterically allowed interactions between a NH moiety and nearby CO groups in a short peptide chain. (Left) Illustration of the competition between local conformational preferences (C_5 interaction, C_7 H-bond) and secondary structures (C_{10} H-bond in a β-turn or a 3_{10} helix, C_{13} bond in a α helix). (Right) Two possible so-called "π H-bonds" of a NH moiety with a nearby aromatic residue R.

(ii) In natural peptides,[11−13,28−31] in contrast, the natural termini of the peptides are kept intact, with the inherent end effects, specific to the C- and N-termini in the gas phase, namely, the presence of powerful H-bond donor and acceptor groups (NH_2 and COOH). The relevance of these gas-phase data to biology can, however, be questioned, since termini are usually charged (zwitterionic forms) in solution. As for modified peptides, short natural peptides like Phe-Gly-Gly, Trp-Gly, Trp-Gly-Gly have also been investigated[11,13,28,29,31] by the IR/UV double-resonance technique, and the structure of the conformers has been identified by comparison with theoretical predictions. Besides these small species, spectra of larger species have also been reported, in particular the FDASV[12] pentapeptide, gramicidin molecules of different types A−D and S,[13] and the sleep-inducing nonapeptide DSIP.[31] Besides these neutral species, charged species have also been the object of numerous investigations, owing to their interest in particular because these species are actually encountered in solution. In this case, the effect of the charge (protonated or cationized species) is quite important and triggers specific polarization effects, like stabilization of zwitterionic forms.[32−36] This topic, however, is beyond the scope of the present study.

† Part of the "Roger E. Miller Memorial Issue".

* Corresponding author: e-mail michel.mons@cea.fr.

10.1021/jp070681l CCC: $37.00
Published on Web 05/27/2007

As far as interpretation of spectroscopic data is concerned, two very different approaches have been proposed and applied so far. First, small structures, on which quantum chemical calculations are still possible at both a decent level of theory and a reasonable computational cost, and with a conformational landscape of still manageable complexity, have been studied: often experimental data, which provide the number of H bonds present in the structure, enable spectroscopists to limit the number of conformations to investigate theoretically.[7,10,37] Such small biomimetic molecules are indeed quite suitable to a "bottom-up" approach, which uses data on smaller species to infer predictions on the larger ones. Jet-cooled species are especially well suited to such an approach since only the most stable conformers are usually observed, even if no chain larger than three residues was documented so far. The case of charged species, with their mobile proton at room temperature, is probably more difficult to treat even if dynamical quantum calculations become now feasible on these species.[38] Alternatively, starting from large species enables one to study functional biomolecules rather than biologically relevant models only.[11−13,31] However, in spite of the resolved or partly resolved character of the spectra reported, no *conformational* assignment has been made so far as soon as the neutral peptide exhibits more than five residues.

In our attempt to understand vibrational spectroscopy of peptides, we have so far concentrated on providing evidence for the intrinsic folding of the chains into secondary structures like β-turns or 3_{10} helices.[7] Our aim is to provide a reliable identification of the spectral signatures of secondary structures, in order to help, in a second step, the identification of the folding structures of larger species, either capped or natural ones. In this line we have investigated model peptides formed with a noncoded achiral amino acid, aminoisobutyric acid (Aib), that is, α-dimethylglycine. This residue is known to induce in the condensed phase (namely, in crystals and nonpolar solutions) the formation of incipient 3_{10} helical structures in short capped homopeptides.[39−42] These structures are stabilized by the presence of C_{10} H-bonds taking place between distant NH and CO groups along the chain (Figure 1) and correspond actually to a succession of β-turns along the chain. In these homopeptides, the type of turn is either I/I′ or III/III′: one molecule of each handedness (unprimed/primed) is observed in the crystal elementary cell. Types I and III are topologically very close. They can be considered as two versions of the same turn feature. Type III, with identical dihedrals (φ, ψ) for each residue (typically −60°, −30°), is consistent with the extended quasi-periodic structure of the 3_{10} helix.[43] Type I, instead, is a slightly distorted version of III, with a single C_{10} H-bond, adapted to an isolated β-turn rather than the helical form. Both forms exist in two helicities, right- or left-handed, the latter being identified by primed labels.

In the gas phase, the structural effects of the presence of Aib in the backbone have been investigated in capped dipeptides. It has recently been shown[25] that Aib combined with a natural L-conformation Phe residue strongly favors the formation of β-turns over alternative conformations, like 2_7 ribbons. Thus two types of turns, type I and II′ turns, could be isolated in a supersonic expansion for the Aib-L-Phe backbone.[25] These preferences are ascribed to the destabilization of the possible C_7 H-bonds due to steric effects between the backbone and the methyl groups of the Aib side chain,[44,45] which shifts the competition between C_7 and C_{10} bonds in favor of the latter. Another gas phase study on the Aib-containing capped dipeptide, Z-Aib-L-Pro-NHMe (Z = benzyloxycarbonyl), has shown theoretically that the type III structure is stable and is actually the global minimum, followed by a type I structure, 2 kcal/mol higher.[27] In spite of these predictions, however, the form observed experimentally in the supersonic expansion is not a β-turn but an open form with a strong C_7 interaction on the proline residue, suggesting the existence of subtle competition between C_7 and C_{10} interactions.

Owing to the general trends of the Aib residue, the investigation of an Aib-based peptide seemed quite interesting in order to ascertain the conclusions of a previous supersonic expansion study[23] on Ala-based tripeptides, namely, (i) the spontaneous formation of an incipient 3_{10} helix ($C_{10}-C_{10}$ conformation) in the Ac-Ala-Phe-Ala-NH_2 molecule and (ii) its competition with C_7-C_{10} forms in Ac-Ala-Ala-Phe-NH_2.

The present paper reports an experimental investigation on a series of three chemically protected peptides based on the same Ac-$(Aib)_3$-NH_2 (Ac = acetyl) tripeptide, in which one Aib residue is substituted by the aromatic phenylalanine (Phe) residue, which bears the ultraviolet chromophore needed to perform IR/UV double resonance experiments. As a major outcome, the main conformer found when Phe stands in the central position shows a great similarity (in terms of both UV and IR spectroscopy) to that of the Ac-Ala-Phe-Ala-NH_2 molecule. The two H-bonds observed experimentally enabled us to restrict considerably the number of conformations of interest to investigate theoretically. Quantum chemistry calculations have been carried out on best candidate structures as well as on remarkable conformations in order to document the relationship between a gas-phase scale of H-bond strengths and their IR signatures. A convergent set of evidence, based on energetic, IR, and UV spectroscopic data, finally enables us to conclude the formation of an incipient 3_{10} helix in this system.

2. Methods

Experimental. The pulsed molecular beam setup has been described in detail elsewhere.[18,24,46] Peptides, purchased from Altergen, were synthesized by the Fmoc technique and used without further purification. Liquid-phase chromatography (LPC) indicated above 80% purity for all three samples. Pellets were made by compressing a mixture of graphite and sample powders (50 mg) and then were cut or filed in order to prepare a fresh surface. The pellet is fixed onto a motor-powered carriage enabling a back-and-forth motion of the surface parallel to itself. The ensemble is fixed close to the nozzle piece of a 10 Hz operating pulsed valve (General Valve), so that the surface stands about 1 mm off the nozzle axis (nozzle orifice diameter 350 μm). The output of the second harmonic of a Nd:YAG laser (Minilite Continuum) is sent to the surface through an optical fiber, whose end, located 3 mm away from the pellet surface, delivers pulses of a few millijoules, leading to a superficial vaporization of the peptide sample. The laser-desorbed molecules are then entrained by a argon gas pulse (backing pressure 6 bar) driven by the pulsed valve, which expands in a first vacuum chamber and is then skimmed before entering a second chamber equipped with a time-of-flight mass spectrometer (TOF MS). Resonant two-photon ionization (R2PI) spectra and IR/UV double resonance spectra were carried out by collecting the ion signal resulting from the interaction of the laser lights with the peptide molecules after mass selection at the TOF MS detector. Peptide molecules were photoionized by the output of an excimer-pumped (Lambda-Physik EMG 200) dye laser (Lambda-Physik FL 2002E). The mass-selected ion signal was acquired and averaged over 100 laser shots in a LeCroy digital oscilloscope as function of the frequency of the laser scanned

and then transferred to the computer and processed. In the IR/UV experiments, the IR radiation is mildly focused onto the molecular beam ($f \sim 500$ mm) and sent typically 50 ns before the UV light. The IR radiation (2.8−3.2 μm) is generated as the idler of a Nd:YAG-pumped $LiNbO_3$ OPO (Euroscan, line width ~ 1 cm^{-1}) and is scanned by tilting simultaneously the crystal and an intracavity Pérot-Fabry plate (free spectral interval 32 cm^{-1}). A typical energy of 1−3 mJ/pulse could be obtained in the IR range scanned, with a smoothly decreasing intensity profile in the low-frequency part, except in the 3465−3500 cm^{-1} region where the OPO emission vanishes due to an intense IR absorption in the crystal.

For the IR/UV spectra, the IR laser is scanned while the IR-induced depletion of one well-defined conformer is probed by the UV laser tuned on a transition of the species considered. When the IR laser is scanned, the "IR on" and "IR off" signals are measured with a PC-controlled shutter. Their difference is then normalized by the "IR off" signal, in order to minimize the effects of long-term fluctuations in the desorption system leading to relative depletion signals. No correction for spectral variations of the IR or UV intensity is applied.

Theoretical. Quantum chemistry calculations of remarkable conformations were performed by the pseudospectral method with the JAGUAR program package.[47] The conformations considered have been chosen primarily within those conformations, based on combinations of C_7 and C_{10} H-bonds,[7] capable of matching the H-bonding pattern measured experimentally (presence of two H-bonds). However, remarkable structures encountered previously in capped dipeptides or other tripeptides have also been considered. These conformations were first fully optimized at the B3LYP/6-31+G(d) level. Then, for each configuration, harmonic vibrational frequencies were calculated at the same level of theory. The NH stretch frequencies obtained were then scaled by 0.960, a factor optimized from the fit of experimental frequencies on smaller species.[24] Intensities can be calculated with the JAGUAR package, but the computation times are rather long because of the numerical computation of the potential derivatives. Previous results on smaller species[7] have shown that the strength of the IR transitions is not a critical parameter for the assignment, for two reasons: first, it is difficult to extract reliable experimental intensities because the IR bands recorded under double resonance conditions are often saturated, and second, there is clear correlation between the band intensity and the strength of the corresponding H-bond (and hence the spectral shift). These two reasons, the lack of reliability of the intensity information and its redundancy with the spectral data, greatly weakens the interest of the calculated IR absorption intensities, which were eventually not computed.

Finally, in order to provide reliable energy calculations, electronic correlation must be taken into account.[21,24] For this purpose, single-point energy calculations were performed at the LMP2/6-31+G(d) level on the B3LYP/6-31+G(d) geometries, according to a calculation strategy validated on smaller species.[24] Unless explicitly stated, the chiral residues considered in the present work are in a L-conformation.

3. Experimental Results

Comparison between the Three Aib-Based Capped Tripeptides. Ac-Phe-Aib-Aib-NH_2, Ac-Aib-Phe-Aib-NH_2, and Ac-Aib-Aib-Phe-NH_2 have all been investigated by R2PI. However, the mass selection carried out in the TOF MS enabled us to detect the nominal mass ions (376 amu) only in the case of the Ac-Aib-Phe-Aib-NH_2 molecule. In the two other cases, the 376 amu mass channel was not observed: only a 291 amu signal was detected, which corresponds to the nominal mass of capped Aib-Phe dipeptides. In both cases, the R2PI spectrum obtained from this 291 amu signal was identical to that recorded previously for the respective Ac-Aib-Phe-NH_2 and Ac-Phe-Aib-NH_2 molecules (on their nominal mass channel 291 amu). Owing to the differences in the LPC signals of the di- and tripeptides, all synthesized by the same company, we conclude that laser desorption of tripeptides exhibiting two adjacent Aib residues suffers from elimination of a part of the molecule during the process (rearrangement in the neutral during the desorption process). The mass loss corresponds to a methacrylamide molecule, whose intrinsic stability might favor the process. As a consequence, the present spectroscopic study is actually limited to the sole Ac-Aib-Phe-Aib-NH_2 molecule.

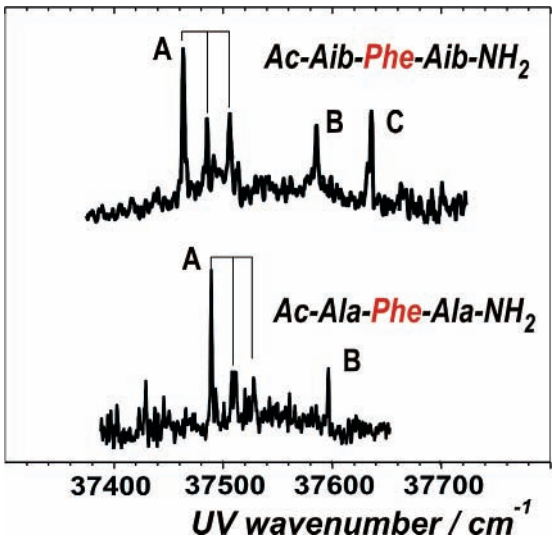

Figure 2. Mass-selected ($m = 376$ amu) R2PI spectra of Ac-Aib-Phe-Aib-NH_2 in the origin region of the near-UV absorption of the phenyl ring. Also shown (lower trace) is the spectrum of Ac-Ala-Phe-Ala-NH_2.[23] Three band systems, labeled A−C, are observed for Ac-Aib-Phe-Aib-NH_2. The origin or the A progression is 37 463 ± 3 cm^{-1}; B and C are blue-shifted by +122 and +173 cm^{-1} respectively. The A origin of Ac-Aib-Phe-Aib-NH_2 is found to be very close to that of Ac-Ala-Phe-Ala-NH_2 by 26 cm^{-1}; that of B, by 10 cm^{-1} only.

UV Spectra. The R2PI spectrum of Ac-Aib-Phe-Aib-NH_2 in the origin region of the near-UV absorption of the phenyl ring is shown in Figure 2. Investigation was focused on the region where previous peptides studied were observed.[7] The mass-selected spectrum ($m = 376$ amu) is composed of a limited number of bands, suggesting a small number of conformers simultaneously present in the jet.

Mass Spectra. When TOF spectra are recorded for the different band systems A−C of the R2PI spectrum, three different patterns are obtained (Figure 3). Besides the nominal 376 mass channel, additional mass channels were detected: mass 332 (loss of a mass 44 moiety) is detected when pumping band A; mass peaks 332 and 291 with B; and mass peaks **394** and 332 with C. In the case of bands A and B, the 332 amu mass is the major apparent fragmentation channel.

As seen above, the daughter ions observed can originate either from ion fragmentation or from photoionization of neutral molecular reaction products formed during desorption.

The origin of the 332 peak is quite clear. The 44 amu mass loss corresponds to the classic elimination of the stable neutral CH_2NO radical by an ionized alkylamide (methacrylamide, 2-methylpropanamide, or 2,2-dimethylpropanamide).[48] The alternative explanation, namely, decarboxylation (loss of CO_2 by the ion), although very likely with a natural peptide (COOH

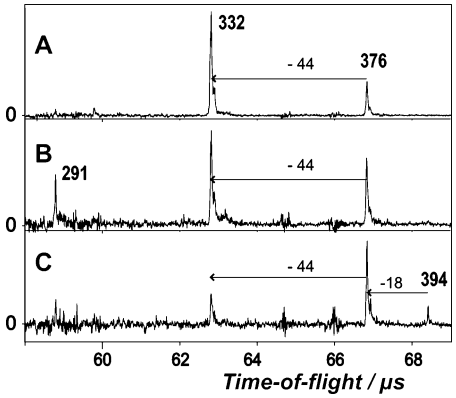

Figure 3. Time-of-flight mass spectra obtained after pumping the bands A, B, and C (from top to bottom, respectively) of Ac-Aib-Phe-Aib-NH_2 ($m = 376$ amu). Corresponding masses are indicated directly on the spectra. All spectra exhibit an intense 332 amu mass channel, corresponding to a 44 amu loss by the parent ion. The C spectrum clearly bears the signature of a fragmented hydrate. B also exhibits a significant $m = 291$ mass peak. See text for details.

terminus), can be ruled out in a capped peptide because of the large reorganization and further fragmentation it would imply in the ion. As a conclusion, both 332 and 376 mass peaks obtained after pumping of the A and B UV bands originate from the photoionization of the parent molecule Ac-Aib-Phe-Aib-NH_2.

The C band can also be explained easily: the observation of a high mass peak at 376 + 18 amu pleads for the formation of the 1:1 hydrate in the expansion (from traces of water in the gas inlet), which is expected to fragment easily into its component by photoionization, giving rise therefore to a pattern dominated by the 376 mass channel, accompanied by the 44 amu loss mass channel. The coincidence between a transition of a hydrate and of another conformer of the parent molecule, however, cannot be excluded.

In contrast, the case of the peak at 291 amu seen from the B band is less obvious. It corresponds indeed to the mass of a neutral molecule that can be formed during the expansion, either Ac-Aib-Phe-NH_2 or Ac-Phe-Aib-NH_2. It can also originate from elimination of a methacrylamide molecule by the ion, as with the two other Aib-based tripeptides, but at a much lesser extent. Due to the minor character of this mass channel, we did not pursue further investigations.

Comparison with the Ala-Based Tripeptide. Apart from the C feature, the spectrum of Ac-Aib-Phe-Aib-NH_2, with its strong A band accompanied by vibronic features at +22 and +43 cm^{-1}, and the isolated, blue-shifted B band is strikingly similar to that of the Ac-Ala-Phe-Ala-NH_2 molecule (also reproduced in Figure 2). Both A-based band systems are very close, the Aib-based molecule being red-shifted by only 26 cm^{-1} relative to the Ala species.

IR Spectroscopy. Reliable IR/UV double-resonant spectra could be carried out only on the most intense band (A) of the UV spectrum of Ac-Aib-Phe-Aib-NH_2. The corresponding IR spectrum (Figure 4) in the amide A region (NH stretches) exhibits four relatively narrow bands (the larger bandwidth is smaller than 15 cm^{-1}), each of them being assigned to the stretching motion of a NH oscillator of the molecule. No reliable spectrum could be carried out from the B band, but a systematic measurement of eventual depletions of the B signal when the IR bands of A were pumped was negative, showing that band B belongs to another, less populated conformer. No IR spectrum was carried out from the C band, but, providing that a better signal-to-noise ratio is obtained, such a piece of information,

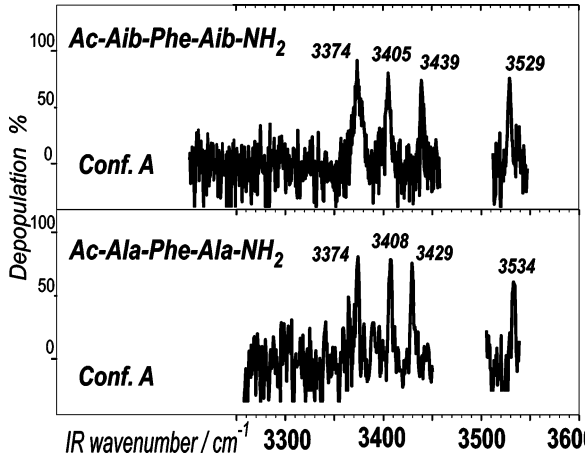

Figure 4. IR/UV double resonance spectrum in the amide A region of conformer A of Ac-Aib-Phe-Aib-NH_2, obtained by probing the UV origin band of the A system. The ion signal was collected in the 332 amu fragment ion channel, which is the most intense ion channel present in the mass spectrum (Figure 3) because of an extensive ionic fragmentation of Ac-Aib-Phe-Aib-NH_2 (see Mass Spectra section). The spectral gap in the 3470−3500 cm^{-1} region is due to an undesired absorption in the crystal of the IR source. The spectrum of conformer A of the Ala-based related compound, Ac-Ala-Phe-Ala-NH_2, already published in ref 23, is also shown for the sake of comparison (bottom panel).

in particular in the OH stretch region of water, should allow us to confirm this band belongs to a hydrate.

Previous studies on shorter peptides carried out in our group have demonstrated that a qualitative picture of the H-bonding network of the molecule can already be drawn from basics of the IR spectroscopy.[7] We have demonstrated that the NH frequency was an accurate indicator of the type of interaction undergone by the corresponding NH moiety: free amide NH stretches are usually found in the 3450−3480 cm^{-1} range (which turns out to be the blind region of our OPO). A red shift from this region is the spectral evidence for a perturbed NH oscillator: The 3415−3450 cm^{-1} range, for instance, will indicate involvement in a C_5 interaction with the CO of the same residue or in a π H-bond with a nearby aromatic ring. More pronounced red shifts will most likely correspond to H-bonds of the C_{10} or C_7 type. In addition, the amide terminal group, rather than a methyl amide group, provides crucial additional information about the involvement of this NH_2 group in the H-bonding and the strength of the corresponding H-bond.[7] The indication stems from the vibrational coupling between the two NH oscillators of the terminal amide $CONH_2$, which causes the symmetric (red) and asymmetric (blue) components of the NH_2 stretch doublet to remain correlated. This correlation has been found to hold for a wide range of NH environments.[7]

These considerations enable us to assign the IR spectrum of Figure 4 to the presence of two rather weak H-bonds (3374 and 3405 cm^{-1}), accompanied by a π H-bond (3429 cm^{-1}). The NH_2 antisymmetric band frequency, relatively high at 3529 cm^{-1}, indicates the involvement of the NH_2-terminal group in the H-bonding, through a weak H-bond, probably that responsible for the band at 3405 cm^{-1}. The missing fifth band should be assigned to a free NH bond, whose frequency should be in the blind region of our IR OPO, as often found so far in these systems.[7,18−24]

Once again comparison with the main conformer A of Ac-Ala-Phe-Ala-NH_2 is quite interesting: the two spectra indeed exhibit very similar patterns, in terms of both frequencies and intensities.

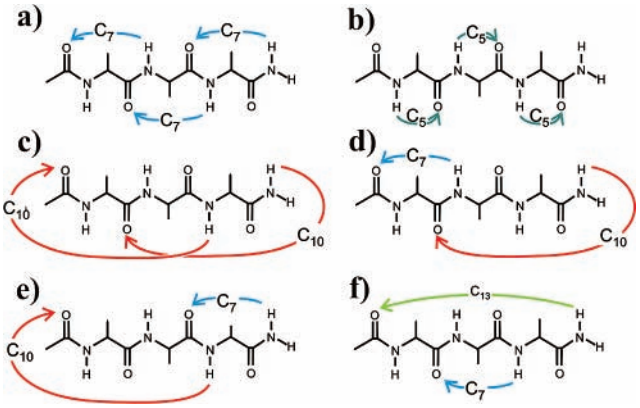

Figure 5. Schemes of the H-bonding networks in the six conformational families sampled in the present theoretical study.

4. Calculations and Discussion

Conformational Selection. Owing to the complexity of the conformational landscape, no extensive exploration of the surface has been carried out. Instead, we have focused our interest on conformations exhibiting two H-bonds as well as on other remarkable conformations (Figure 5). These conformations are as follows: (i) a juxtaposition of local preferences (C_7 and C_5 interactions), $C_5-C_5-C_5$ and $C_7-C_7-C_7$; (ii) combinations of secondary structures, involving different types of C_{10} bonds (β-turns): owing to the preferences due to Aib in Aib-Phe dipeptides (type I or type II′)[25] and due to Phe in Phe-Aib (type I), I−I and II′−I $C_{10}-C_{10}$ combinations have been considered; (iii) a mixture of local preferences (C_7) and secondary structures (β-turns/C_{10} bonds), C_7-C_{10} and $C_{10}-C_7$, with respectively type I and II′ C_{10}; and (iv) extended γ-turns (C_7 with a parallel C_{13} H-bond). Conformations having a unique isolated C_{13} H-bond as well as incomplete 2_7 ribbons have been disregarded because of the strong energetic penalty due to missing H-bonds compared to structures saturated in H-bonds.

In all these conformations, the orientation (anti, gauche +, or gauche −) of the Phe side chain (described by the χ_{Phe} dihedral angle) was chosen in order to establish an NH$-\pi$ H-bond between the phenyl ring and the nearby available NH moieties, since previous studies revealed that, as soon as such bonds are possible for a certain backbone shape, they form spontaneously under cold conditions, with a net energy gain on the order of 2 kcal/mol.[24] The geometries resulting from B3LYP/6-31+G(d) optimizations are summarized in Table 1, namely, the dihedral angles associated with each residue, Aib(1), Phe, and Aib(2).

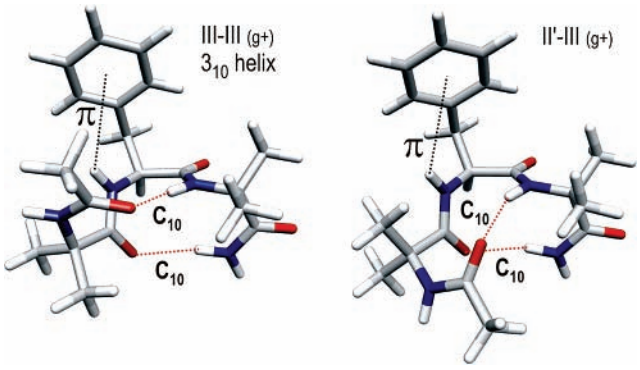

Figure 6. B3LYP/6-31+G(d) equilibrium structures of the two $C_{10}-C_{10}$ (g+) conformations of Ac-Aib-Phe-Aib-NH_2, showing the two C_{10} H-bonds and the NH$-\pi$ interaction responsible for their stability. The helical form is found to be the most stable, followed by the II′-III form at 1.8 kcal/mol.

Energetics and Structure. Among all the conformations calculated, the most stable form is the 3_{10} helical $C_{10}-C_{10}$ conformation, followed by the other $C_{10}-C_{10}$ form (Figure 6) and the γ-turn ($C_7//C_{13}$ form).

The two $C_{10}-C_{10}$ forms correspond to successive β-turns, respectively III−III and II′−III, since the initial type I turns converged toward type III structures, which are more compatible with a quasi-periodic structure. The ideal type III turn, indeed, exhibits the same dihedral angles for the first and the second residue of the turn (−60°, −30°; −60°, −30°), instead of (−60°, −30°; −90°, −0°) in type I. In this respect, the Aib-based helical tripeptide is much closer to an ideal 3_{10} helical structure than its Ala-based counterpart, whose second β-turn (C terminal side) is clearly of type I (see Table 1, bottom). The third conformation, γ-turn, is composed of a central relatively strong C_7 H-bond, accompanied by a parallel C_{13} H-bond linking the two ends of the molecule.

Amide A IR Spectroscopy. The stick spectra obtained (Figure 7) exhibit a large diversity, which shows the great interest of the IR spectroscopy in the amide A region as a pertinent structural diagnostic. The spectral region below 3415 cm^{-1} enables a straightforward classification of the H-bond networks as a function of the bond strengths. The weaker bonds are usually due to C_{10} H-bonds but also to C_5 interactions as encountered in the $C_5-C_5-C_5$ form. The strongest bonds are due to combinations of bonds, especially C_7-C_{10} and $C_7-C_7-C_7$, in which the same peptide moiety acts as a proton donor for one H-bond and as an acceptor for another. The resulting cooperative effects lead to red shifts down to 3280 cm^{-1}.

TABLE 1: B3LYP/6-31+G(d) Optimized Structures for Selected Conformations of Ac-Aib-Phe-Aib-NH_2[a]

conformation[b]	$\varphi_{Aib}^{(1)}$	$\psi_{Aib}^{(1)}$	φ_{Phe}	ψ_{Phe}	$\varphi_{Aib}^{(2)}$	$\psi_{Aib}^{(2)}$	χ_{Phe}	$\Delta E_{B3LY\ P}$	ΔE_{MP2}	ΔZPE_{B3LYP}	$\Delta E_{MP2} + \Delta ZPE_{B3LYP}$
Ac-Aib(1)-Phe-Aib(2)-NH_2											
$C_5-C_5-C_5$ (a) [β-strand]	−180	−178	−156	145	−180	178	−173	0.83	4.39	−0.59	3.79
$C_{10}-C_{10}$ III−III (g+) [3_{10} helix]	−60	−31	−73	−6	−63	−28	58	0	0	0	0
$C_{10}-C_{10}$ II′−III (g+)	53	−131	−73	−10	−71	−20	56	1.02	1.62	0.22	1.84
$C_7//C_{13}$ (g+) [γ-turn]	−62	−31	−82	60	65	33	41	0.74	2.14	−0.20	1.94
$C_{10}-C_7$ II′−γ_D (g+)	−62	−24	−99	9	74	−57	50	1.76	3.03	0.24	3.27
C_7-C_{10} γ_L−III (g+)	−74	62	−72	−18	−66	−22	67	0.09	3.71	0.13	3.84
$C_7-C_7-C_7$ (g−) [2_7 ribbon]	−73	50	−86	70	−74	54	−63	0.05	3.87	0.31	4.17
Ac-Ala-Phe-Ala-NH_2											
$C_{10}-C_{10}$ III−I (g+) [3_{10} helix]	−68	−21	−74	−1	−100	3	57				0[c]
$C_{10}-C_{10}$ II′−I (g+)	55	−127	−75	−1	−100	3	56				1.63[c]

[a] See section 4 for the conformational choice. The relative orientations of the peptide units on both sides of each residue are described by the φ, ψ dihedral angles. They are given in degrees, as well as the orientation of the Phe side chain χ_{Phe}. Relative energies (ΔE) at different levels are given: B3LYP/6-31+G(d) energies, single-point LMP2/6-31+G(d)//B3LYP/6-31+G(d) energies, B3LYP/6-31+G(d) zero-point vibrational energies, and ZPE-corrected single-point MP2 energies. All energies, given in kilocalories per mole, are expressed relative to the most stable structure found. For the sake of comparison, the corresponding calculated data for the two $C_{10}-C_{10}$ conformations of Ac-Ala-Phe-Ala-NH_2 are also given, taken from the Supporting Information of ref 23. [b] Corresponding secondary structure is given in brackets. [c] Single point MP2/6-31+G(d)//B3LYP/6-31+G(d).

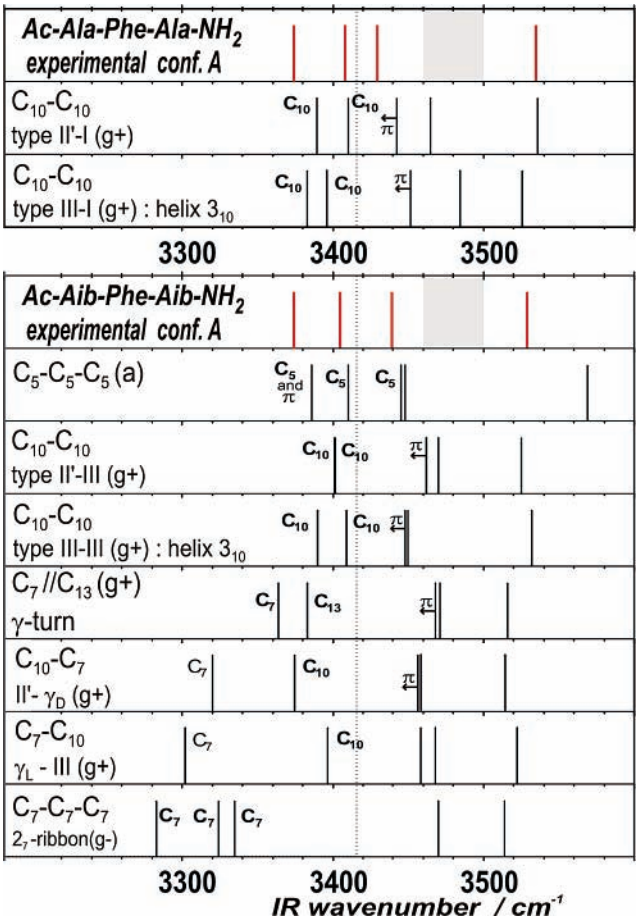

Figure 7. (Lower panel) B3LYP/6-31+G(d) calculated stick spectra of the selected conformations of Table 1 (see section 4) in the amide A region (NH stretches) compared to the experimental frequencies of the main conformer A. Calculated harmonic frequencies are scaled by a factor of 0.960.[24] Bands are labeled according to the nature of the interaction involved. The dotted line (3415 cm^{-1}) indicates a typical upper limit for H-bond spectral signatures. Shaded areas correspond to a blind region of the IR source. Arrows indicate the systematic underestimation of the π interaction at the B3LYP/6-31+G(d) level (see text). (Upper panel) Corresponding experimental and calculated data for the two $C_{10}-C_{10}$ conformations of Ac-Ala-Phe-Ala-NH_2, adapted from the Supporting Information of ref 23.

Assignment of the A Form of Ac-Aib-Phe-Aib-NH_2. Among all the calculations carried out, the best fit to the experimental spectrum of A is provided by conformations having two weak H-bonds, namely, the two $C_{10}-C_{10}$ conformations.

The $C_5-C_5-C_5$ form, whose spectrum bears a striking resemblance to that of $C_{10}-C_{10}$ III−III, can be excluded because of the mismatch in the blue part of the spectrum: its unperturbed NH_2 moiety leads to a rather blue NH_2 antisymmetric band. Such a similarity between a weak H-bond, like C_{10}, and a C_5 bond, especially when cooperative effects are favored by a β-strand structure, was already noticed in dipeptides.[20,21] A significant cooperative effect together with its combination with a NH$-\pi$ interaction seems to explain the relatively large red shift of the redmost band for a C_5 interaction.

Conversely, the γ-turn-like conformation $C_7//C_{13}$ must be excluded because its NH_2 moiety is engaged in the C_{13} H-bond, as indicated by the significantly red-shifted NH_2 stretch antisymmetric band.

The other forms, all possessing C_7 local arrangements, exhibit at least one strongly red-shifted band, which cannot fit the experimental data.

Between the two $C_{10}-C_{10}$ forms, the most stable structure, the helical one (Figure 6), provides the best fit: the H-bonding pattern is better reproduced by this latter form as well as the antisymmetric stretch of the amino group. This goes with the better prediction of the weaker C_{10} H-bond, since this latter corresponds to the symmetric NH_2 stretch component (Table 2). The red shift of the stronger C_{10} bond is found to be slightly underestimated (by 15 cm^{-1}), which seems to be a systematic trend of the B3LYP/6-31+G(d) level of theory, already encountered in other peptide conformations exhibiting two H-bonds (C_7-C_7, for instance[20]). As far as the NH$-\pi$ H-bonds are concerned, it is well documented that their red shift is typically underestimated by 10−15 cm^{-1}.[7,20,22,24] This is indicated on the corresponding bands of Figure 7 by arrows pointing toward the red. When this is taken into account, the helical form provides better agreement for the typical π H-bond signature at 3439 cm^{-1}.

TABLE 2: Spectroscopic (Amide A) IR Data of Conformer A of Ac-Aib-Phe-Aib-NH_2 Compared to Scaled Harmonic Frequencies[a]

conformation	NH(Aib$^{(1)}$)	NH(Phe)	NH(Aib$^{(2)}$)	NH_2sym	NH_2anti
experimental	not obs	3439	3374	3405	3529
$C_5-C_5-C_5$ (a)	3410	3445	3386	3448	3569
$C_{10}-C_{10}$ III−III (g+)	**3450**	**3448**	**3390**	**3409**	**3532**
$C_{10}-C_{10}$ II′-III (g+)	3470	3462	3401	3402	3525
$C_7//C_{13}$ (g+)	3450	3446	3353	3428	3545
$C_{10}-C_7$ II′−γ_D (g+)	3458	3456	3374	3320	3514
C_7-C_{10} γ_L−III (g+)	3468	3301	3458	3396	3522
$C_7-C_7-C_7$ (g−)	3470	3283	3335	3324	3514

[a] IR frequencies are given in reciprocal centimeters. Harmonic frequencies (scaling factor 0.960) were calculated for the series of optimized conformations of Table 1. The best fit to experimental values is provided by the helical structure (shown in boldface type).

All these features coincide with those observed on the similar Ac-Ala-Phe-Ala-NH_2 system[23] as illustrated in Figure 7. These independent studies leading to the same conclusion provide strong evidence for the observation of the same 3_{10} helical form, in spite of minor specificities linked to the residue side chains (III−III vs III−I types).

Low-Frequency Bands. Finally, we show that UV spectra, namely, the study of Franck−Condon (FC) active low-frequency modes, can also provide an interesting piece of supporting information. FC activity reflects the change in equilibrium geometry between the ground and the excited S_1 state. There are a few examples in the literature[24,49,50] of a fair agreement between the excited-state frequencies as measured in UV spectra and the low frequencies calculated by quantum chemistry techniques (for the ground state). The agreement is due partly to the large similarities between the two electronic states and partly to the small values of these frequencies, which implies that the absolute differences between S_1 and S_0 frequencies remain small, even if it can amount to 10% or more in relative values.

Measured and predicted values on protected dipeptides[25] exhibiting significant FC activity (β-turns in particular) already show a good agreement: The most FC-active vibrations experimentally observed find a counterpart among the low-frequency modes calculated (Table 3): calculated harmonic frequencies are expected to be of the same order of magnitude, slightly too large because of the strong anharmonicity anticipated for low-frequency modes. As an example, the two type-II′ β-turns (Ac-D-Ala-Phe-NH_2 and Ac-Aib-Phe-NH_2)[25] exhibit a low-frequency mode in the 16−17 cm^{-1} region, which matches fairly well a calculated mode, involving mainly a shearing motion of the phenyl ring relative to the backbone. The agreement is not as good with the type I β-turn of Ac-Aib-Phe-NH_2, but the calculated frequency (too large) remains nevertheless as close as 2 cm^{-1} to its experimental counterpart.[25]

TABLE 3: Frequencies of the Franck−Condon Active Low-Frequency Modes[a] Compared to the Calculated (Unscaled) Frequencies[b]

molecule	exp	calc		mode assignment
Ac-D-Ala-Phe-NH_2	conf B′	β-turn		type II′ g+
	17/33[c]	***19***		shearing/stretch of phenyl ring/backbone
		30		libration of phenyl/backbone
		44		libration of phenyl/backbone
		48		backbone distortion
Ac-Aib-Phe-NH_2	conf B	β-turn		type I g+
		16		shearing of phenyl/backbone
	29	***27***		libration of phenyl/backbone and/acetyl
		43		libration of phenyl/backbone and/acetyl
		54		distortion of the central peptide bond
Ac-Aib-Phe-NH_2	conf B′	β-turn		type II′ g+
	16	***18***		shearing of phenyl/backbone
	26	***29***		libration of phenyl/backbone
		45		libration of phenyl/backbone
Ac-Ala-Phe-Ala-NH_2	conf A	III−III g+	II′−III g+	
		23	18	libration of phenyl/backbone + backbone
	22	***24***	27	libration of phenyl/acetyl and/backbone
		28	29	backbone
	39	40	41	libration of phenyl/backbone
		51	46	libration of phenyl/backbone
Ac-Aib-Phe-Aib-NH_2	conf A	III−III g+	II′−III g+	
		16	15	shearing of phenyl/backbone
	22/43[c]	***23***	***20***	libration of phenyl/backbone
		30	***22***	global torsion of the helix
		37	38	torsion helix + phenyl
		46	47	libration cycle/backbone

[a] Observed in the R2PI spectra of capped di- and tripeptides [b] Low-frequency modes (<50 cm^{-1}) were calculated at the B3LYP/6-31+G(d) level of theory for selected conformations and are given in reciprocal centimeters. A rough description of the calculated modes is given, in particular the motion of the phenyl ring relative to the backbone, expected to be crucial for the FC activity. For the dipeptides, the conformational assignment was obtained independently of the analysis of the low-frequency modes;[25] a fair agreement is observed. For the tripeptides, the experimental data (present work and ref 23) are compared to the calculated frequencies of the two C_{10}−C_{10} conformations. Calculated data that best fit the experimental values are shown in boldface type (see text). [c] Second member of a progression.

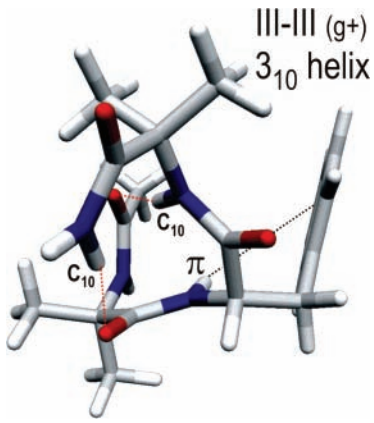

Figure 8. Axis view of the III−III (g+) helical structure from its C terminus, as obtained from B3LYP/6-31+G(d) optimization.

It is therefore tempting to use this fair agreement as an additional hint for the assignments of the C_{10}−C_{10} forms observed, in particular to distinguish between III−III and II′−III combinations. Low-frequency bands are observed in the UV spectra of both Aib- and Ala-based[23] tripeptide chains, with the frequencies +22/+43 cm^{-1} and +22/+39 cm^{-1}, respectively (Figure 2). In the Aib-based tripeptide, the 43 cm^{-1} frequency, slightly smaller than twice the first one, suggests a progression in a 22 cm^{-1} mode, corroborated by the absence of calculated low-frequency mode in this region. The +22 cm^{-1} experimental frequency is not very useful for the conformational assignement, since both III−III and II′−III combinations exhibit a calculated frequency in this range, at 23 and 22 cm^{-1}, respectively.

In the case of the Ala-based tripeptide, however, the +22/+39 cm^{-1} bands suggest two different modes. In contrast to the previous molecule, two calculated frequencies lie in the 22 cm^{-1} range for the III−III form but none for the II′−III form (Table 3). No discrimination arises from the 39 cm^{-1} frequency since for both forms one mode can account for observation. From this comparison it appears that, among the two C_{10}−C_{10} structures, the III−III helical structure provides better agreement for the +22 cm^{-1} mode in the Ala-based peptide. This observation, independent of the energetic or IR studies, is an additional supporting argument in favor of the formation of helical forms in the capped Ala- and Aib-based tripeptides.

5. Conclusion

The aim of the present work on Aib-based capped peptides was to take advantage of the helicogenic properties of Aib in order to document the competition between the different types of backbone folding. An Aib residue within a peptide backbone is indeed supposed to favor C_{10} H-bonds over smaller C_7 folds, eventually resulting in easy formation of 3_{10} helical folding. Unfortunately, because of poor stability of the Aib peptides under laser desorption conditions, the competition between C_7 and C_{10} bonds could not be investigated as thoroughly as expected. The issue of the formation of incipient helical forms, however, has been addressed for the Ac-Aib-Phe-Aib-NH_2 molecule and the similarities with the Ac-Ala-Phe-Ala-NH_2 species have been discussed. We provide here a consistent set of data on these two molecules, encompassing UV and IR spectra of the main conformer and calculated vibrational modes in the low-frequency and amide A regions, which enables us to confirm the spontaneous helical folding property of a capped tripeptide chain in the gas phase. This gas-phase helical folding (Figure 8) can be considered as the isolated counterpart of structures encountered in crystals of model Aib-based peptides.[39−42]

Beyond this assignment, the present work, in particular the synthesized IR spectra, illustrates the diversity of spectral IR signatures among the several conformations expected a priori,

even in such a small and simple molecule as a capped tripeptide without polar side chains. It also emphasizes that radically different structures can exhibit rather close spectral features, suggesting the crucial need for simultaneous complementary spectroscopic diagnostics, involving signatures in the NH and CO stretch regions, in the fingerprint region, etc., as well as extensive structural calculations, when larger molecules are targeted.

References and Notes

(1) Pribble, R. N.; Zwier, T. S. *Science* **1994**, *265*, 75 and references therein.
(2) Zwier, T. S. *J. Phys. Chem. A* **2001**, *105*, 8827 and references therein.
(3) Robertson, E. G.; Simons, J. P. *Phys. Chem. Chem. Phys.* **2001**, *3*, 1 and references therein.
(4) Weinkauf, R.; Schermann, J. P.; de Vries, M. S.; Kleinermanns, K. *Eur. Phys. J. D* **2002**, *20*, 309 and references therein.
(5) Dong, F.; Miller, R. E. *Science* **2002**, *298*, 1227 and references therein.
(6) Choi, M. Y.; Miller, R. E. *J. Am. Chem. Soc.* **2006**, *128*, 7320.
(7) Chin, W.; Piuzzi, F.; Dimicoli, I.; Mons, M. *Phys. Chem. Chem. Phys.* **2006**, *8*, 1033 and references therein.
(8) Mons, M.; Piuzzi, F.; Dimicoli, I.; Gorb, L.; Leszczynski, J. *J. Phys. Chem. A* **2006**, *110*, 10921.
(9) Gerhards, M.; Unterberg, C. *Phys. Chem. Chem. Phys.* **2002**, *4*, 1760.
(10) Gerhards, M.; Unterberg, C.; Gerlach, A.; Jansen, A. *Phys. Chem. Chem. Phys.* **2004**, *6*, 2682.
(11) Reha, D.; Valdes, H.; Vondrasek, J.; Hobza, P.; Abu-Riziq, A.; Crews, B.; de Vries, M. S. *Chem.*—Eur. J. **2005**, *11*, 6803.
(12) Abo-Riziq, A.; Bushnell, J. E.; Crews, B.; Callahan, M.; Grace, L.; De Vries, M. S. *Chem. Phys. Lett.* **2006**, *431*, 227.
(13) Abo-Riziq, A.; Crews, B. O.; Callahan, M. P.; Grace, L.; de Vries, M. S. *Angew. Chem., Int. Ed.* **2006**, *45*, 5166.
(14) Gerhards, M.; Unterberg, C.; Gerlach, A. *Phys. Chem. Chem. Phys.* **2002**, *4*, 5563.
(15) Bakker, J. M.; Aleese, L. M.; Meijer, G.; von Helden, G. *Phys. Rev. Lett.* **2003**, *91*, 203003.
(16) Fricke, H.; Gerlach, A.; Gerhards, M. *Phys. Chem. Chem. Phys.* **2006**, *8*, 1660.
(17) Gerlach, A.; Unterberg, C.; Fricke, H.; Gerhards, M. *Mol. Phys.* **2005**, *103*, 1521.
(18) Chin, W.; Mons, M.; Dognon, J.-P.; Piuzzi, F.; Tardivel, B.; Dimicoli, I. *Phys. Chem. Chem. Phys.* **2004**, *6*, 2700.
(19) Chin, W.; Compagnon, I.; Dognon, J. P.; Canuel, C.; Piuzzi, F.; Dimicoli, I.; von Helden, G.; Meijer, G.; Mons, M. *J. Am. Chem. Soc.* **2005**, *127*, 1388.
(20) Chin, W.; Dognon, J. P.; Canuel, C.; Piuzzi, F.; Dimicoli, I.; Mons, M.; Compagnon, I.; von Helden, G.; Meijer, G. *J. Chem. Phys.* **2005**, *122*, 054317.
(21) Chin, W.; Dognon, J. P.; Piuzzi, F.; Tardivel, B.; Dimicoli, I.; Mons, M. *J. Am. Chem. Soc.* **2005**, *127*, 707.
(22) Chin, W.; Piuzzi, F.; Dognon, J. P.; Dimicoli, I.; Mons, M. *J. Chem. Phys.* **2005**, *123*, 084301.
(23) Chin, W.; Piuzzi, F.; Dognon, J. P.; Dimicoli, I.; Tardivel, B.; Mons, M. *J. Am. Chem. Soc.* **2005**, *127*, 11900.
(24) Chin, W.; Mons, M.; Dognon, J. P.; Mirasol, R.; Chass, G.; Dimicoli, I.; Piuzzi, F.; Butz, P.; Tardivel, B.; Compagnon, I.; von Helden, G.; Meijer, G. *J. Phys. Chem. A* **2005**, *109*, 5281.
(25) Brenner, V.; Piuzzi, F.; Dimicoli, I.; Tardivel, B.; Mons, M. *Angew. Chem., Int. Ed.* **2007**, *46*, 2463.
(26) Compagnon, I.; Oomens, J.; Bakker, J.; Meijer, G.; von Helden, G. *Phys. Chem. Chem. Phys.* **2005**, *7*, 13.
(27) Compagnon, I.; Oomens, J.; Meijer, G.; von Helden, G. *J. Am. Chem. Soc.* **2006**, *128*, 3592.
(28) Hünig, I.; Kleinermanns, K. *Phys. Chem. Chem. Phys.* **2004**, *6*, 2650.
(29) Cohen, R.; Brauer, B.; Nir, E.; Grace, L.; de Vries, M. S. *J. Phys. Chem. A* **2000**, *104*, 6351.
(30) Abo-Riziq, A. G.; Crews, B.; Bushnell, J. E.; Callahan, M. P.; De Vries, M. S. *Mol. Phys.* **2005**, *103*, 1491.
(31) Bakker, J. M.; Plutzer, C.; Hunig, I.; Haber, T.; Compagnon, I.; von Helden, G.; Meijer, G.; Kleinermanns, K. *ChemPhysChem* **2005**, *6*, 120.
(32) Oh, H. B.; Lin, C.; Hwang, H. Y.; Zhai, H. L.; Breuker, K.; Zabrouskov, V.; Carpenter, B. K.; McLafferty, F. W. *J. Am. Chem. Soc.* **2005**, *127*, 4076.
(33) Kapota, C.; Lemaire, J.; Maitre, P.; Ohanessian, G. *J. Am. Chem. Soc.* **2004**, *126*, 1836.
(34) Lucas, B.; Gregoire, G.; Lemaire, J.; Maitre, P.; Glotin, F.; Schermann, J. P.; Desfrancois, C. *Int. J. Mass Spectrom.* **2005**, *243*, 105.
(35) Oomens, J.; Sartakov, B. G.; Meijer, G.; Von, Helden, G. *Int. J. Mass Spectrom.* **2006**, *254*, 1.
(36) Oomens, J.; Polfer, N.; Moore, D. T.; van der Meer, L.; Marshall, A. G.; Eyler, J. R.; Meijer, G.; von Helden, G. *Phys. Chem. Chem. Phys.* **2005**, *7*, 1345.
(37) Valdes, H.; Reha, D.; Hobza, P. *J. Phys. Chem. B* **2006**, *110*, 6385.
(38) Marinica, D. C.; Gregoire, G.; Desfrancois, C.; Schermann, J. P.; Borgis, D.; Gaigeot, M. P. *J. Phys. Chem. A* **2006**, *110*, 8802.
(39) Benedetti, E.; Bavoso, A.; Diblasio, B.; Pavone, V.; Pedone, C.; Crisma, M.; Bonora, G. M.; Toniolo, C. *J. Am. Chem. Soc.* **1982**, *104*, 2437.
(40) Mammi, S.; Rainaldi, M.; Bellanda, M.; Schievano, E.; Peggion, E.; Broxterman, Q. B.; Formaggio, F.; Crisma, M.; Toniolo, C. *J. Am. Chem. Soc.* **2000**, *122*, 11735.
(41) Crisma, M.; Bisson, W.; Formaggio, F.; Broxterman, Q. B.; Toniolo, C. *Biopolymers* **2002**, *64*, 236.
(42) Crisma, M.; Moretto, A.; De Zotti, M.; Formaggio, F.; Kaptein, B.; Broxterman, Q. B.; Toniolo, C. *Biopolymers* **2005**, *80*, 279.
(43) Richardson, J. S. *Adv. Protein Chem.* **1981**, *34*, 167.
(44) Aleman, C. *J. Phys. Chem. B* **1997**, *101*, 5046.
(45) Bisetty, K.; Catalan, J. G.; Kruger, H.; Perez, J. J. *J. Mol. Struct. (THEOCHEM)* **2005**, *731*, 127.
(46) Piuzzi, F.; Dimicoli, I.; Mons, M.; Tardivel, B.; Zhao, Q. *Chem. Phys. Lett.* **2000**, *320*, 282.
(47) JAGUAR 5.5, Schrodinger LLC, Portland, OR, 1991−2003 ed.
(48) NIST Chemistry WebBook, http://webbook.nist.gov/chemistry/.
(49) Hockridge, M. R.; Robertson, E. G.; Simons, J. P. *Chem. Phys. Lett.* **1999**, *302*, 538.
(50) Schmitt, M.; Feng, K.; Boehm, M.; Kleinermanns, K. *J. Chem. Phys.* **2006**, *125*, 9.